Developmental and Comparative Immunology 67 (2017) 107–116

Contents lists available at ScienceDirect

Developmental and Comparative Immunology

journal homepage: www.elsevier.com/locate/dci

Evolution of *Ciona intestinalis* Tumor necrosis factor alpha (*Ci*TNFα): Polymorphism, tissues expression, and 3D modeling

Aiti Vizzini [1], Maria Giovanna Parisi [1], Laura Cardinale, Lelia Testasecca, Matteo Cammarata*

Dipartimento di Scienze e Tecnologie Biologiche, Chimiche e Farmaceutiche, Via Archirafi 18, Palermo, Italy

ARTICLE INFO

Article history:
Received 21 June 2016
Received in revised form
4 November 2016
Accepted 5 November 2016
Available online 6 November 2016

Keywords:
TNF
Ciona intestinalis
DGGE
Polymorphism
Gene expression

ABSTRACT

Although the Tumor necrosis factor gene superfamily seems to be very conserved in vertebrates, phylogeny, tissue expression, genomic and gene organization, protein domains and polymorphism analyses showed that a strong change has happened mostly in invertebrates in which protochordates were a constraint during the immune-molecules history and evolution.

RT PCR was used to investigate differential gene expression in different tissues. The expression shown was greater in the pharynx.

Single-nucleotide polymorphism has been investigated in *Ciona intestinalis* Tumor necrosis factor alpha (CiTNFα) mRNA isolated from the pharynx of 30 ascidians collected from Licata, Sicily (Italy), by denaturing gradient gel electrophoresis (DGGE). For this analysis, *Ci*TNFα nucleotide sequence was separated into two fragments, TNF-1 and -2, respectively, of 630 and 540 bp. We defined 23 individual DGGE patterns (named 1 to 10 for TNF-1 and 1 to 13 for TNF-2). Five patterns for TNF-1 accounted for <10% of the individuals, whereas the pattern 13 of TNF-2 accounted for >20% of the individuals. All the patterns were verified by direct sequencing. Single base-pair mutations were observed mainly within COOH-terminus, leading to 30 nucleotide sequence variants and 30 different coding sequences segregating in two main different clusters. Although most of the base mutations were silent, four propeptide variants were detected and six amino acid replacements occurred within COOH-terminus. Statistical tests for neutrality indicated negative selection pressure on signal and mature peptide domains, but possible positive selection pressure on COOH-terminus domain. Lastly we displayed the in silico 3D structure analysis including the *Ci*TNFα variable region.

1. Introduction

The study of genes and genomes evolution allows us to understand the role of different evolutionary forces, including natural selection. The structure and composition of a gene are inherited from the organism's ancestors, so it may be that various driving forces cause the change of structural and functional aspects of a gene, allowing adaptation to the environment.

Genetic variability is a potential mechanism for evolutionary change and adaptation as it can give a selective advantage to organisms in various environmental conditions. It is considered a driver of recognition capability of self from non-self, the basic condition for the evolution of metazoans.

The Tumor Necrosis Factor Superfamily (TNFS) is involved in many cellular signaling pathways such as inflammation, apoptosis, lymphocyte homeostasis and tissue development (Bodmer et al., 2002; Ware, 2003). The TNFSF ligands are type II membrane proteins with an intracellular N-terminus and an extracellular C-terminus. The majority of these ligands are bound to membrane and several of these ligands encode proteolytic cleavage sites able to generate soluble forms holding biological activity (Locksley et al., 2001). The TNF homology domain (THD) is located in the C terminus and is weakly conserved (20–30%) between ligand members. The signature THD is composed of 10 β-strands, which ultimately fold to form a compact "*jellyroll*" topology. Three monomers join to form a stable conical trimeric protein, which is then able to initiate signaling through its respective receptor(s) (Bodmer et al., 2002). TNF is produced mainly from macrophages

* Corresponding author.
E-mail address: matteo.cammarata@unipa.it (M. Cammarata).
[1] The first two authors contributed equally.

http://dx.doi.org/10.1016/j.dci.2016.11.005
0145-305X/

but also from other cell types including lymphoid cells, mast cells, endothelial cells and neurons (Galli et al., 2011).

The *C. intestinalis* inflammatory response to several irritants appears to be composed of a complex reactions set. The cellular reactions in the tunic involve hemocyte infiltration, hemocyte and epidermis activities, vacuolization and cell disruption, while cell products can contribute to form capsule components and/or cause a tunic wound (Parrinello et al., 2015). In this response the involvement of the pharynx, as the main immune-competent organ, has been disclosed by a lipopolysaccharide (LPS) challenge that upregulates innate immunity genes and transcription activation genes.

In *Ciona intestinalis,* a Tumor Necrosis Factor-alpha (TNFα)-like gene challenged with bacterial lipopolysaccharide (LPS) was cloned and sequenced (Parrinello et al., 2008).

A larger cell-bound cytokine form in the hemocytes and a smaller one in the serum hemolymph suggest roles in both local and systemic responses. After LPS inoculation, *in situ* hybridization with CiTNFα riboprobe and immunohistochemistry with a specific antibody showed an increased number of positive amebocytes with large granules, contained in the pharynx vessels, in the connective tissue lining the tunic and vessel epithelium, as well as in circulating hyaline amebocytes and granulocytes. TNFα is also expressed during the swimming larval phase of development (Parrinello et al., 2010). *Ci*TNFα-like protein appears to be a type II transmembrane protein with an extracellular C-terminal domain that may be glycosylated and released as a soluble cytokine upon proteolytic processing (Bodmer et al., 2002). The recombinant protein of *Ciona Savignyi* TNF homolog showed potential cytotoxic activity against L929 cells confirming a potential role in morphogenesis, inflammation and immunity of ascidians TNFs.

Denaturing gradient gel electrophoresis (DGGE) is an electrophoresis separation method based on differences in melting properties of double stranded DNA fragments (Fisher and Lerman, 1979). It is one of the most efficient and widely applied methods for detection of nucleotide differences through an increasing denaturant gradient of urea formamide (Abrams and Stanton, 1992; Lerman and Beldjord, 1998). DGGE has been applied to different biological purposes from genetic mutations (Sheffield et al., 1989) to bacterial diversity (Muyzer et al., 1993; Van der Gucht and Vandekerckhove, 2005) and genetic polymorphism (Ge et al., 1999; Cantet et al., 2012). Sensitivity of DGGE allows one single base substitution to be detected by adding a 40 base-pair G + C rich sequence (called GC clamp) to the forward specific PCR primer used in amplification (Sheffield et al., 1989).

Here, we further characterized *Ci*TNFα of *Ciona intestinalis* from the phylogeny standpoint, tissues expression and 3D structure. We also applied DGGE technology to demonstrate the diversity of *Ci*TNFα mRNAs segregating in 30 ascidian specimens. Cloning and sequencing of multiple PCR-generated TNF-1 and TNF-2 fragments established the relationships between patterns and nucleotide sequences, point mutations and deduced propeptide sequences. We also performed several tests for neutrality suggesting negative selection pressure on signal and mature peptide domains, but possible positive selection pressure on the COOH-terminus domain.

2. Materials and methods

2.1. Tunicates

Ascidians were collected from Licata, Sicily (Italy) maintained in aerated sea water at 15 °C and fed every second day with a marine invertebrate diet (Coraliquid, Sera Heinsberg, Germany). The ascidian tunic surface was cleaned and sterilized with ethyl alcohol. A suitable amount (200 mg/ascidian) of pharynx, ovary, intestine and stomach tissues was excised and immediately soaked in RNAlater tissue collection (Ambion, Austin, TX), and stored at −80 °C. Although the systematic of this species has been reexamined and the Mediterranean species defined as *Ciona robusta* (Brunetti et al., 2015), we used *Ciona intestinalis* until definitive clarification of the Mediterranean species had been established.

2.2. Bionformatic analysis

Gene structure was checked on the Ensembl genome browser, and domain conservation was predicted by SMART software (http://smart.embl-heidelberg.de/). Similarity searches were performed using the BLAST algorithm (www.ncbi.nlm.nih.gov/blast/). Sequences were subjected to multiple alignments using CLC workbench 6.4. Phylogenetic analyses were conducted using a maximum likelihood (ML) analysis with default parameters and using MEGA6 for Neighbor Joining method (NJ) after 1000 bootstrap iterations.

The accession numbers are as follows: DQ070246.1 (*Dicentrarchus labrax* TNF-α), AJ413189.2 (*Sparus aurata* TNF-α), AF276961.1 (*Salvelinus fontinalis* TNF), AB183467.1 (Danio *rerio* TNF-α), X54000.1 (*Felis catus* TNF-α), NM_001003244.4 (*Canis lupus familiaris* TNF), NM_000594.3 (*Homo sap*iens TNF), AY427675.1 (*Rattus norvegicus* TNF-α), KC713805.1 (*Mustela putorius furo* TNF-α), X55966.1 (Ov*is aries* TNF-αa), NM_001280615.1 (*Tursiops truncatus* TNFa), JQ793636.1 (*Anguilla japonica* TNF-α), JQ807663.1 (Th*unnus thynnus* TNF-α), NM_001128107.1 (*Ciona intestinalis* TNF-α), EU216599.1 (*Ciona savignyi* TNF), ID ENSCSAVP00000019575) predicted *Ciona savignyi* TNF-2), NM_165735.4 (*Drosophila melanogaster* eiger A), NM_206069.3 (*Drosophila melanogaster* eiger B), U77036.1 (*Cavia porcellus* TNF-α), AB298595.1 (*Xenopus laevis* TNF-α), HM581661.1 (Halio*tis diversicolor* TNF-α), HQ696609.1 (*Ctenopharyngodon idella* TNF-α), EU863217.1 (Halio*tis discus discus* TNF-α), KM079078.1 (An*drias davidianus* TNF-α), HQ174260.1 (*Crassostrea gigas* TNF).

Protein structural models were developed with SWISS-MODEL and Swiss-PdbViewer (Guex and Peitsch, 1997; Arnold et al., 2006; Schwede et al., 2003) by using human TNF superfamily ligand TL1A 2re9.1.B as a template. The *cis*-regulatory elements were identified using the web REGRNA tool.

2.3. Total RNA extraction and cDNA synthesis

Total RNA was isolated from the respective ovary, intestine and stomach tissues of four ascidians and from the pharynx tissues of 30 ascidians by using an RNAqueousTM-Midi Kit purification system (Ambion) and reverse-transcribed by the Cloned AMV First-Strand cDNA Synthesis Kit (Invitrogen).

2.4. Real-time PCR

Tissue expression of the *Ci*TNFα gene was examined by real-time PCR analysis with the Sybr-Green method (Applied Biosystems 7500 real-time PCR system). Tissue expression was performed in a 25-μl PCR containing 2 μl cDNA converted from 250 ng total RNA, 300 nM *Ci*TNFα forward (5-GCCTCCCATAGACCGTTGTTAA-3′) and *Ci*TNFα reverse (5′-CGGGA CACCTTCAGCACAT-3′) primers, 300 nM actin forward (5′-TGATGTTGCCGCACTCGTA-3′) and actin reverse (5′-TCGACAATGGATCCGGT-3′) primers, and 12.5 μl Power Sybr-Green PCR Master Mix (Applied Biosystems). The 50 cycles of the two-step PCR program consisted of initial polymerase activation for 3 min at 95 °C followed by a denaturing step at 95 °C for 15 s, and then annealing/extension was carried out at 60 °C for 45 s when the fluorescent signal was detected. Each set of samples was run three times, and each plate contained quadruplicate cDNA samples and

negative controls. The specificity of amplification was tested by real-time PCR melting analysis. To obtain sample quantification the 2−ΔΔCt method was used, and the relative changes in gene expression were analyzed as described in the Applied Biosystems Use Bulletin N.2 (P/N 4303859). The amount of *Ci*TNFα transcript from the various tissues was normalized to actin in order to compensate for variations in input RNA amounts. Relative *Ci*TNFα expression was determined by dividing the normalized value of the target gene in each tissue by the normalized value obtained from the untreated tissue.

2.5. Denaturing gradient gel electrophoresis (DGGE)

*Ci*TNF sequence was divided in two parts: a 630 bp fragment (TNF-1) and a 540 bp fragment (TNF-2). The amplification was performed using GC clamp forward primers 5′-CGCCC GCCGC GCCCC GCGCC CGGCC CGCCG CCCCC GCCCG-3'. Two TNF fragments were amplified using primers showed in Table 1. PCR was performed by AmpliTaq Gold DNA Polymerase (Applied Biosystems). Amplification comprised 2 min of initial denaturation at 95 °C, followed by 30 cycles consisting of 95 °C for 30 s, 60 °C for 1 min, 72 °C for 1 min, and a final extension at 72 °C for 7 min. Expected size of amplicons was checked by 1% agarose gel electrophoresis. Polymorphism of amplicons was then analyzed by DGGE on a Vertical Electrophoresis DCODE system (Bio-Rad) with 6% (w/v) polyacrylamide gels and denaturizing gradient from 20% to 80%. The 100% denaturizing solution was composed of 7M urea and 40% formamide (v/v). Samples were prepared by adding 7 μl of 6X loading dye solution (Fermentas; 0.03% bromophenol blue, 0.03% xylen cyanol, 60% glycerol, 60 mM EDTA in 10 mM Tris−HCl pH 7.6) to 7 μl of PCR amplicon. DGGE was performed in Tris-acetate-EDTA buffer (TAE: 40 mM Tris-base, pH 7.4 with HCl, 20 mM glacial acetic acid, 1 mM EDTA) at 60 °C for 16 h at 80 V constant voltage. Gels were stained for about 30 min in the dark with 3 μl concentrated 10,000 × SybrGold (Molecular Probes) diluted in 30 ml TAE, and washed for 15 min in TAE. They were photographed using the UV Imager Gel Doc XR (BioRad) using the SYBR filter. Band patterns were analyzed on the basis of densitometry calculated for each lane through AlphaView gel acquisition software (Alpha Innotech).

The DGGE gel obtained indicated that each pattern produced a single dominant band that appeared at a different position in the gel, indicating the potential of the primers to resolve different patterns. Some patterns revealed additional bands, but the intensities of these bands were always much lower than the intensity of the dominant band. We sequenced the bands obtained with the primer set that accounted for the higher value of total band intensity.

The common pattern among the different samples was defined as “profile”.

Finally, PCR products were cloned into the pCRIIvector (TAcloning Kit, Invitrogen) and sequenced. Suitable amounts of lyophilized samples were analyzed by BMR Genomics (Padua, Italy) to determine nucleotide sequences.

2.6. Analysis of cDNA and deduced amino acid sequences

The nucleotide sequences obtained were translated into propeptides (http://www.expasy.ch/tools/dna.html) and resulting amino acid sequences were compared using Multalin (http://multalin.toulouse.inra.fr). Site-by-site frequency spectrum-based statistical assays were used to test the hypothesis of polymorphisms within loci being neutral: Tajima's D (Tajima, 1989), Fu and Li's D and Fu and Li's F (Fu and Li, 1993), available at http://www.ub.es/dnasp/.

Table 1
TNF Primers used for DGGE product amplification and/or direct sequencing.

Gene	Primer	Direction	Primer sequence (5′-3′)
TNF-1	TNF1F	Forward	AATATGCAGTCCTTGTCGT
	TNF1R	Reverse	CCATATGTGTCAGCATACAA
TNF-2	TNF2F	Forward	GACAGTACTTGGTTTACATGC
	TNF2R	Reverse	TCTATTTATAACATAAA

3. Results

3.1. Gene organization and phylogenesis of the TNF

TNF mRNAs from invertebrates and vertebrates were used to construct a phylogenetic tree to revise the evolutionary dynamic of the TNF gene. The TNF phylogenetic tree showed three main clusters: the first two included the chordata that may be further classified into sub-clusters of fish and vertebrates, and the third included the protochordate. A more variable cluster included the invertebrate group with an unusual, but uncertain form of TNF from *C. savignyi* that is currently in the draft data bank but not verified by cloning or mRNA presence. Finally, an additional cluster seems to have been formed by two longer sequences of *A. japonica and A. davidianus.* Results showed that the TNF gene effected very big changes in invertebrates including protochordates, but resulted conservative in vertebrates (Fig. 1).

*Ci*TNFα genomic and domain organization and comparison with Human, *D. rerio* TNFα and *D. melanogaster* EigerA genes were performed (Fig. 2A and B). *Ci*TNFα and *D. melanogaster* EigerA genes contained 7 exons and 6 introns and the longer cds, Human and *D. rerio* TNFα genes, contained 4 exons and 3 introns. The highest content in exons of invertebrates resulted in proteins with a higher amino acid content in invertebrates compared to vertebrates (Fig. 2A).

A computational analysis was performed using the REGRNA tool to identify *cis*-regulatory elements in the 3′UTR of *C. intestinalis*, Human, *D. rerio* TNFα and *D. melanogaster* EigerA (Fig. 2C). Searches identified in *D. melanogaster* EigerA and CiTNFα an Interferon-γ-activated inhibitor of translation (GAIT) element and a Musashi binding element (MBE), two for *C. intestinalis* and three for *D. melanogaster*; in *D. rerio* TNFα a GAIT element and an ARE element were present with a shorter 3′UTR organization; in Human TNFα the 3′UTR region contained an AU rich element (ARE2), GAIT and TNF elements (Fig. 2C).

3.2. Differential gene expression in different tissues

The spatial expression pattern of *Ci*TNFα in adult *Ciona intestinalis* was investigated by quantitative real time PCR analysis of total RNA samples from different tissues (pharynx, ovary, stomach, intestine). Expression was detected in all examined tissues. As shown in Fig. 3, the expression was greater in pharynx and intestine than in stomach and ovary.

3.3. mRNA polymorphism revealed by DGGE

Amplicons obtained respectively with GC-TNF1-F and TNF1-R primers, GC-TNF2-F and TNF2-R primers were subjected to DGGE electrophoresis (data not shown).

The reproducibility of the fingerprints was estimated by quantifying the intensities of the same bands obtained in independent PCR and DGGE analyses (Diez et al., 2001).

Analyses of the DGGE patterns that shared identical nucleotide sequences were restricted to one profile. We thus obtained ten different profiles for TNF-1 (Fig. 4 A) and thirteen profiles for TNF-2 (Fig. 4 B), a phenomenon also observed for myticin C (Costa et al.,

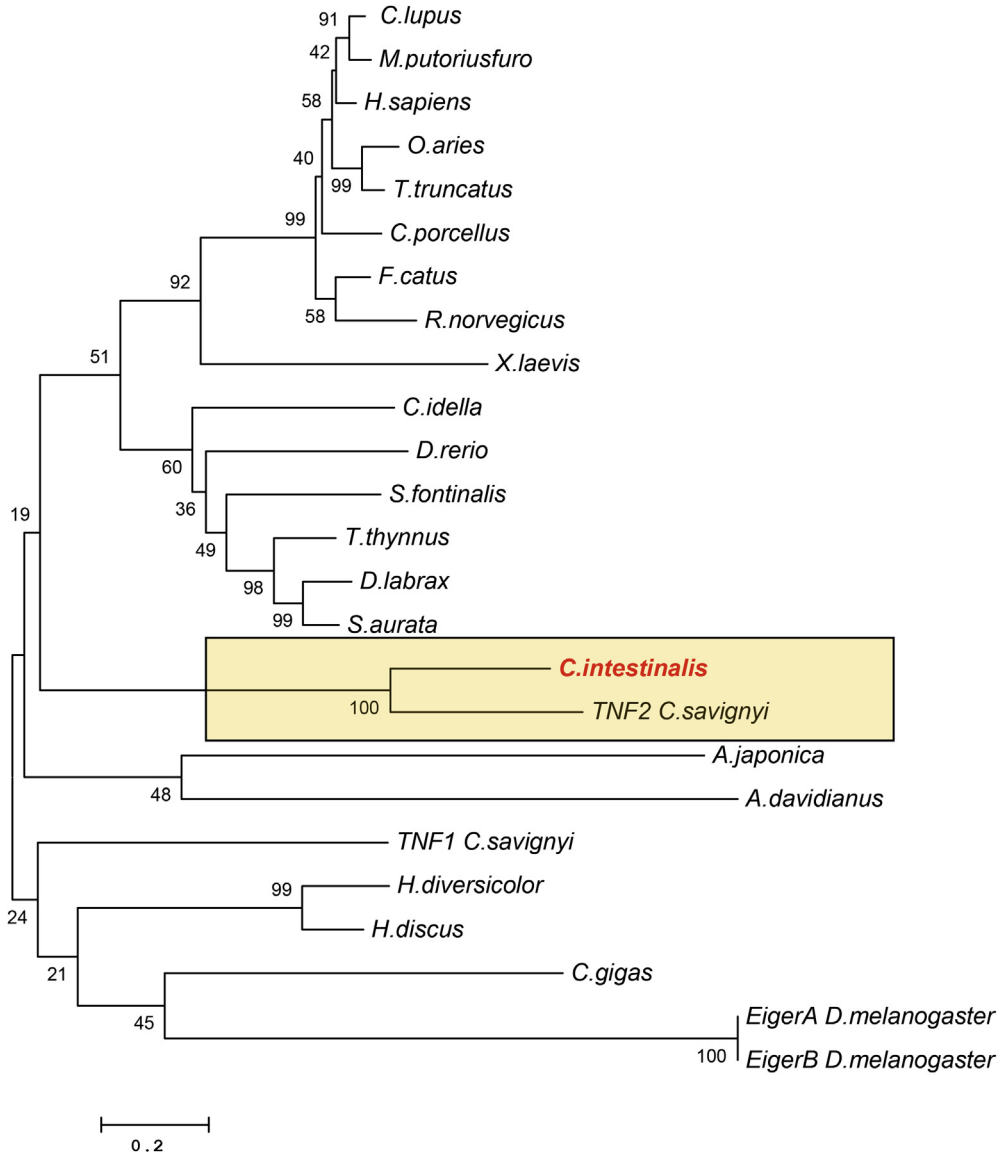

Fig. 1. Phylogenetic tree of vertebrate and invertebrate members of TNF family proteins. The evolutionary history was inferred using the Neighbor-Joining method. The optimal tree with the sum of branch length = 10.476 is shown. The percentage of replicate trees in which the associated taxa clustered together in the bootstrap test (1000 replicates) is shown next to the branches. The tree is drawn to scale, with branch lengths in the same units as those of the evolutionary distances used to infer the phylogenetic tree. The evolutionary distances are expressed as the number of base substitutions per site. Evolutionary analyses were conducted by using MEGA6 software.

2009).

The potential of DGGE for identifying *C. intestinalis* intra-population polymorphism was addressed by sequencing DGGE bands of ascidian cDNA samples.

After DGGE migration, all molecular patterns observed were sequenced and variant sequences in 30 *Ci*TNF-α cds were identified.

3.4. Differences in mRNA and amino acid sequences

We identified 60 mRNAs sequences for TNF-1 and TNF-2, having linked in a unique TNF coding sequence, reducing the number of different complete coding sequences from 60 to 30.

Nucleotide and amino acidic sequences of 30 ascidians were cloned, sequenced and aligned with *Ci*TNF-α (NM_001128107.1), in which 295 aa of 312 were invariant and as little as 5.45% present variability at different levels (Fig. 5, Table 2).

Mutations with an effect on amino acid levels were more numerous within the COOH-terminus (six sites within 281–309 aa, 1.92%) Both the transmembrane domain and propeptide contained few mutations: 3 sites within 1–28 aa and 4 sites within 29–102 aa.

Mutations at nucleotide level occurred with different frequencies, from **low** (one sequence out of the 30 analyzed for nucleotides-20, 36, 49, 226, 617, 916, 917; two sequences out of the 30 analyzed 6.67% for nucleotides-916, 917; three sequences out of the 30 analyzed had about 10% of variability for nucleotides-7, 324, 523, 914, 915, 916, 917, 918), **intermediate** (four sequences out of the 30 analyzed, i.e. 13.33% for nucleotides-304, 307, 308; five sequences out of the 30 analyzed, i.e. 16.67% for nucleotides-914, 916, six sequences out of the 30 analyzed, i.e. 20% for nucleotides-912, 926; seven sequences out of the 30 analyzed, i.e. 23.33% for nucleotides-841, 852; eight sequences out of the 30 analyzed, i.e. 26.67% for nucleotides-403, 873) **to frequent** (13 sequences out of the 30 analyzed, showing 43.33% of variability for nucleotides-501 within the mature peptide region; 27 sequences out of the 30

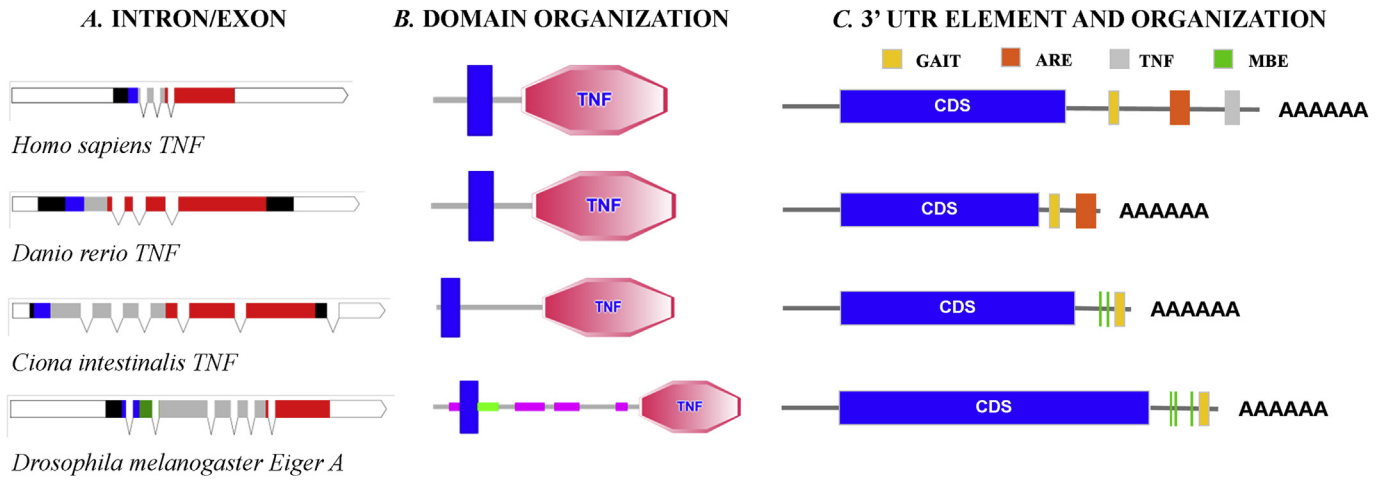

Fig. 2. TNFα gene organization. (A): Comparison of the intron/exon sizes between *Ci*TNFα Human, *D. rerio* TNFα and *D. melanogaster* EigerA genes (introns are reduced) and (B) the related domains organization. The thin line represents the introns and the open boxes indicate the exons of the respective genes. (C): 3′ UTR organization performed using the web REGRNA tool: GAIT (Interferon-γ-activated inhibitor of translation), ARE and ARE2 (AU rich elements), MBE (Musashi binding element), TNF (Tumor Necrosis Factor element).

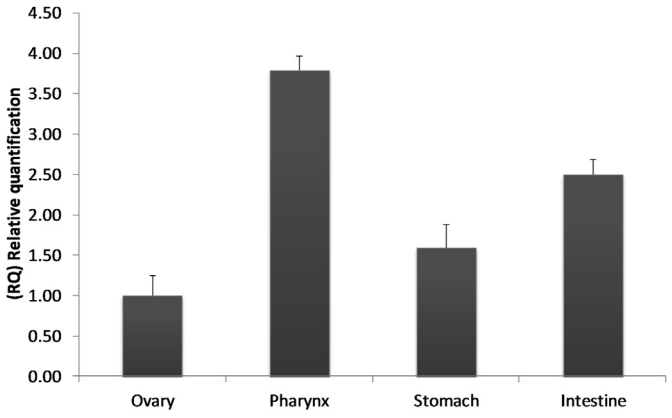

Fig. 3. Tissue expression of *Ci*TNF-α. mRNA expression level is calculated by quantitative real time PCR analysis relative to actin expression and shown as mean ± SD (n = 4).

analyzed, i.e. 90% for nucleotides-204, 289 within the propeptide region).

The transmembrane domain included three mutation points, the propeptide included five mutation points and the mature TNF portion without the C terminus sequence included four mutation points in the amino acid composition. The most frequent mutation (90%) in the coding sequences region (cds) with respect to Genbank cds was found in the propeptide, the two other most frequent mutations (43.33% and 26.67%) were found in the mature peptide. In all cases the modified amino acids maintained the same properties (Table 2). By contrast, the COOH-terminus contained 12 mutation points, one found with a maximum frequency of 26.67% among all the sequences. It was within this COOH-terminus that nine mutation points (841, 852, 912, 914, 915, 916, 917, 918, 926) were located that induced different amino acids. The mutations 916, 917, 918, leading to Glu306, were found in only 10% of the sequences, and only in profile M, which was encountered in only three of the 30 tested TNF. In contrast, the mutation 926, leading to Lys309, was found in three out of 13 patterns (P, U, W), representing 20% of the analyzed sequences. The replacement of a non-polar side chain amino acid (Phe) by acidic and negative charged polar side chain amino acid (Glu) might induce different properties of the COOH-terminus (Fig. 4 and Table 2).

3.5. Selection pressure analysis

To determine whether neutral selection was operating within the codon sites of the *Ci*TNF-α cds variants, several related parameters were defined using three different statistical tests (Table 3). All three tests were in agreement with the hypothesis of negative selection pressure regarding transmembrane domain, propeptide and mature peptide. Only for the C-terminus region did Fu and Li's D and F test value of 1.40 and 1.69 suggest possible positive selection pressure, not clearly confirmed by Tajima's D test. When applied to full cds three different statistical tests indicated possible negative selection pressure, probably mainly influenced by the C-terminus region showing also the major values of variable sites and nucleotide diversity per site.

The nonsynonymous/synonymous mutation ratio (ω) indicated values of $\omega < 1$ for both entire coding sequences and mature peptide analysis of 30 *Ci*TNFa sequences and values of $\omega > 1$ for the transmembrane domain and propeptide (Table 3).

3.6. 3D modeling

A structural homology analysis was carried out using the SWISS-MODEL program. The homology modeling process was performed on the basis of the known crystal structure of human TL1A (2re9B) (e-value 1E-14; QMEAN Z-Score: −3.594, Fig. 6A). Fig. 6 B shows the *Ci*TNF molecular model resulting from superimposition of 106–284 residue sequences that share 21.11% identity. *Ci*TNF holds antiparallel β-sheets organized in a typical "jellyroll" TNF structure. The overlapping between target/template structures is shown in Fig. 6 C. In Fig. 6 D, of particular interest are the positions reported of more frequent aminoacid variable sites including the C-terminal variables aa, all corresponding in a closed and external region.

4. Discussion

Evolution can change the structures and functions of genes in many ways (Wu and McLarty 2012). From the single cell to mammals, the protection against infectious agents has evolved due to the continuously occurring host/parasite relationships (Ballarin and Cammarata, 2016). Key features of the immune responses are the high intrinsic diversity of the molecules of self/non-self recognition, challenge-specific protection and complex regulatory

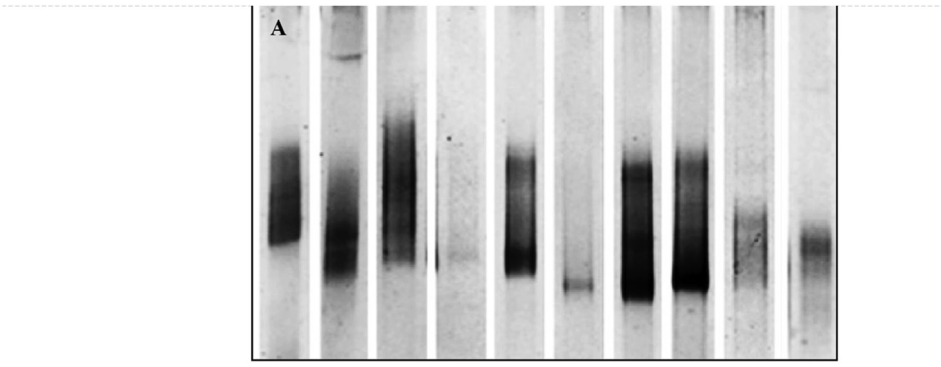

Patterns	A	B	C	D	E	F	G	H	I	J
Frequencies	6.67	6.67	16.67	3.33	10.00	6.67	3.33	13.33	13.33	10.00

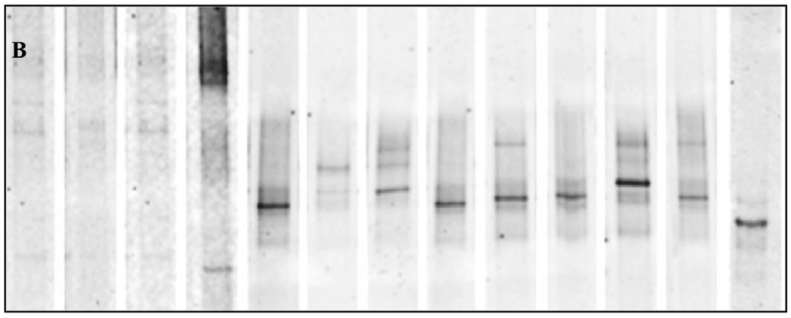

Patterns	K	L	M	N	O	P	Q	R	S	T	U	W	X
Frequencies	10.00	6.67	10.00	3.33	6.67	6.67	6.67	3.33	6.67	3.33	10.00	3.33	20.00

Fig. 4. Different profiles of *Ci*TNF-α mRNA observed by DGGE analysis, and frequencies of occurrence (%) within the population from Licata (AG), Sicily (Italy) (n = 30). (A) 10 profiles for TNF-1 and (B) 13 profiles for TNF-2.

integration.

Ciona intestinalis Tumor Necrosis Factor alpha gene (*Ci*TNFα), which has been previously cloned and sequenced, is expressed either during the inflammatory pharynx response to lipopolysaccharide (LPS) or during the swimming larval phase of development (Parrinello et al., 2008). Granulocytes with large granules and compartment/morula cells are CiTNFα-producing cells in both inflamed pharynx and larvae. Pharynx vessel endothelium also takes part in the inflammatory response. Haemocyte nodules in the vessel lumen or associated with the endothelium suggest the involvement of *Ci*TNFα in recruiting lymphocyte-like cells and promoting the differentiation of inflammatory haemocytes. Specific antibodies against a *Ci*TNFα peptide have identified a 43-kDa cell-bound form of the protein.

In vertebrates, TNF is constitutively expressed by a variety of cells and tissues, including monocytes and macrophages and some endocrine and epithelial cells (Roger et al., 2007). It is rapidly released into circulation by pre-formed intracellular vesicles following a non-conventional leaderless pathway (Benigni et al., 2000), particularly after exposure to toxins and microbial cell wall components and pro-inflammatory mediators in response to stress (Bacher et al., 1998). Here, via real time PCR, we demonstrated that *Ci*TNFα is expressed in various tissues, but preferentially in the pharynx, and less so in the intestine.

To explore the evolutionary dynamic of TNF family genes, TNF mRNAs from invertebrates and vertebrates were used to construct a phylogenetic tree to revise the evolutionary dynamic of TNF gene. The TNF phylogenetic tree showed three main clusters: results indicated that the TNF gene has effected very big changes in invertebrates, but was conservative in protochordates and vertebrates supporting a conserved evolution from a common TNF ancestral gene.

To discover more about evolutionary relationships of TNFs, we performed 3D modeling using TNF molecular models deposited in the databank.

The putative molecular modeling of TNF had a similar “jellyroll” structure to that of human TNF including a β sheet sandwich constructed of antiparallel β strands the core of the jellyroll consists of two sheets of four β strands (Eck and Sprang, 1989). In addition to minor differences in amino acid replacements along the sequence, the major difference occurred on the short insertion in the *Ci*TNF of 10 aa between Glu 132 and Val 133, forming a very short alpha helix. Together with the amino terminal strand, the carboxyl-terminal strand, in which a higher number of “hot” mutation points are present, constitute the first two strands of the inner sheet.

*Ci*TNFα genomic, domain organization and 3′UTR comparative analysis shower a relatively complex gene organization of *Ci*TNFα with 7 exons and 6 introns regarding the vertebrate gene organization. An intriguing 3′UTR gene organization in *Ci*TNFα showed common regions with other vertebrates as an Interferon-γ-activated inhibitor of translation (GAIT) element, but also a Musashi

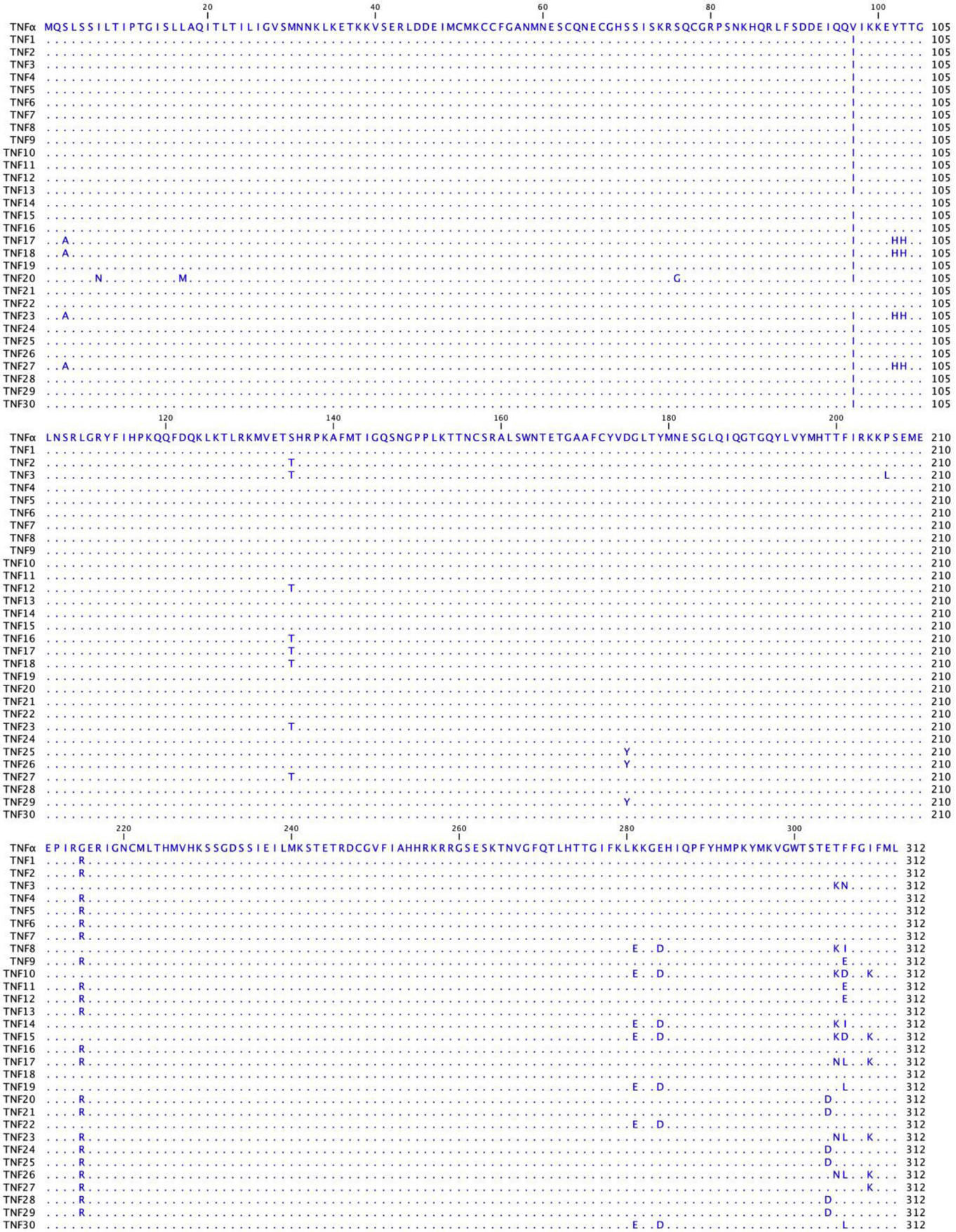

Fig. 5. Multiple comparison of 30 sequences of *Ciona intestinalis* TNF-α. Translated full length sequences of 312 aminoacid residues are aligned with TNF-α (NM_001128107.1). Dot indicates identical aminoacids. Variable aminoacids are indicated in blue.

Table 2
Location, occurrence and nature of nucleotide and amino acid replacements within TNF-α coding sequence. The 3 locations with nucleotide replacements inducing different amino acids are shaded. *Nucleotide from sequence NM_001128107.1.

TNFα	Replacement location	Position in codon*	Alternate nucleotide	Frequency occurrence %	Corresponding aminoacids
1	7	T-1st	G	10.00 %	Ala
transmembrane domain	20	T-2d	A	3.33 %	Asn
	36	T-3rd	G	3.33 %	
84	49	C-1st	A	3.33 %	Met
85	204	C-3rd	T	90.00 %	
	226	A-1st	G	3.33 %	Gly
	289	G-1st	A	90.00 %	Ile
propeptide	304	T-1st	C	13.33 %	His
	307	A-1st	C	13.33 %	His
	308	C-2d	A	13.33 %	His
390	324	C-3rd	T	10.00 %	
391	403	T-1st	A	26.67 %	Thr
	501	A-3rd	C	43.33 %	
	523	G-1st	T	10.00 %	Tyr
	617	C-2d	T	3.33 %	Leu
	643	G-1st	C	70.00 %	Arg
	841	A-1st	G	23.33 %	Glu
	852	A-3rd	T	23.33 %	Asp
	873	T-3rd	C	26.67 %	
	912	A-3rd	C	20.00 %	Asp
mature peptide	914	C-2d	A	16.67 %	Lys or Asn
	915	A-3rd	T or G	10.00 %	Asn
	916	T-1st	C	16.67 %	Leu
			G	10.00 %	Glu
			A or G	6.67 %	Ile or Asp
			A	3.33 %	Asp
	917	T-2d	A	10.00 %	Glu or Asp
			A	6.67 %	
			A	3.33 %	
	918	C-3rd	A	10.00 %	Glu
939	926	T-2d	A	20.00 %	Lys

Table 3
Polymorphism and assays for neutrality in TNF-α variants of *Ciona intestinalis* from Licata, Sicily (Italy). Significant at 0.05% except (*).

	Total cds	Transmembrane domain	Pro-peptide	Mature peptide	COOH-terminus
Domain positions	1–939	1–84	85–390	391–939	841–939
Number of nucleotides per domain	939	84	306	549	99
Number of variable sites (**S**)	26	4	7	15	10
Nucleotide diversity per site (π)	0.00759	0.00523	0.00439	0.00974	0.03783
Nonsyn/syn ratio **(ω)**	−0.65732	1.04270	1.17465	0.40228	0.88812
Neutrality tests					
Tajima's **D**	−0.09538	−1.45103	−0.70968	0.60742	1.53151
Fu and Li's **D***	0.58527	−1.98083	0.57673	1.25846	1.40570*
Fu and Li's **F***	0.43013	−2.11954	0.22074	1.23596	1.68943*

binding element (MBE). The 29-nt structural element, denoted as an IFN-gamma-activated inhibitor of translation (GAIT), has been experimentally demonstrated to be sufficient for translational silencing both in vitro and in vivo (Sampath, 2003). It also has been demonstrated that the MBE sequence was critical for temporal regulation (Charlesworth et al., 2002; Charlesworth et al., 2006), including a possible function on developmental stages.

To investigate genetic variability of CiTNFα specific primers were designed to ensure amplification of full coding regions. Among the 30 ascidians from the Licata population, Sicily, original patterns were identified for TNF-1 and the same number for TNF-2. All patterns shared identical nucleotide sequences were restricted to one profile (10 profiles for TNF-1 and 13 profiles for TNF-2).

In synthesis, we detected multiple alignments that allowed us to identify point mutations showing a high degree of variability in the *Ciona intestinalis* TNF sequences. Both synonymous and non-synonymous mutations were detected in TNF-α domains, suggesting an involvement in molecular functionality.

Proteins with highly variable sequences are not rare in vertebrates (immunoglobulins, MHC and TLR for instance) and have been also reported in ascidians with the fester gene (Nyholm et al., 2006) and a highly polymorphic gene coding for the variable complement receptor-like 1 (vCRL1), structurally similar to vertebrate complement receptors. However, in contrast to vertebrate complement receptors, vCRL1 shows an unprecedented high degree of amino acid variations among various individuals (Kurn et al., 2006).

Proteins with variable sequences have been reported in other invertebrates: sea urchin with TLR (Hibino et al., 2006), Drosophila with TLR (Tauszig et al., 2000), Dscam (Watson et al., 2005), PGRP (Royet et al., 2005) and AMPs (Imler and Bulet, 2005), shrimp with penaeidins (Padhi et al., 2007), gastropods with FREP (Zhang et al., 2004), bivalves with myticin C and Mytilin B (Parisi et al., 2009; Gestal et al., 2007; Pallavicini et al., 2008).

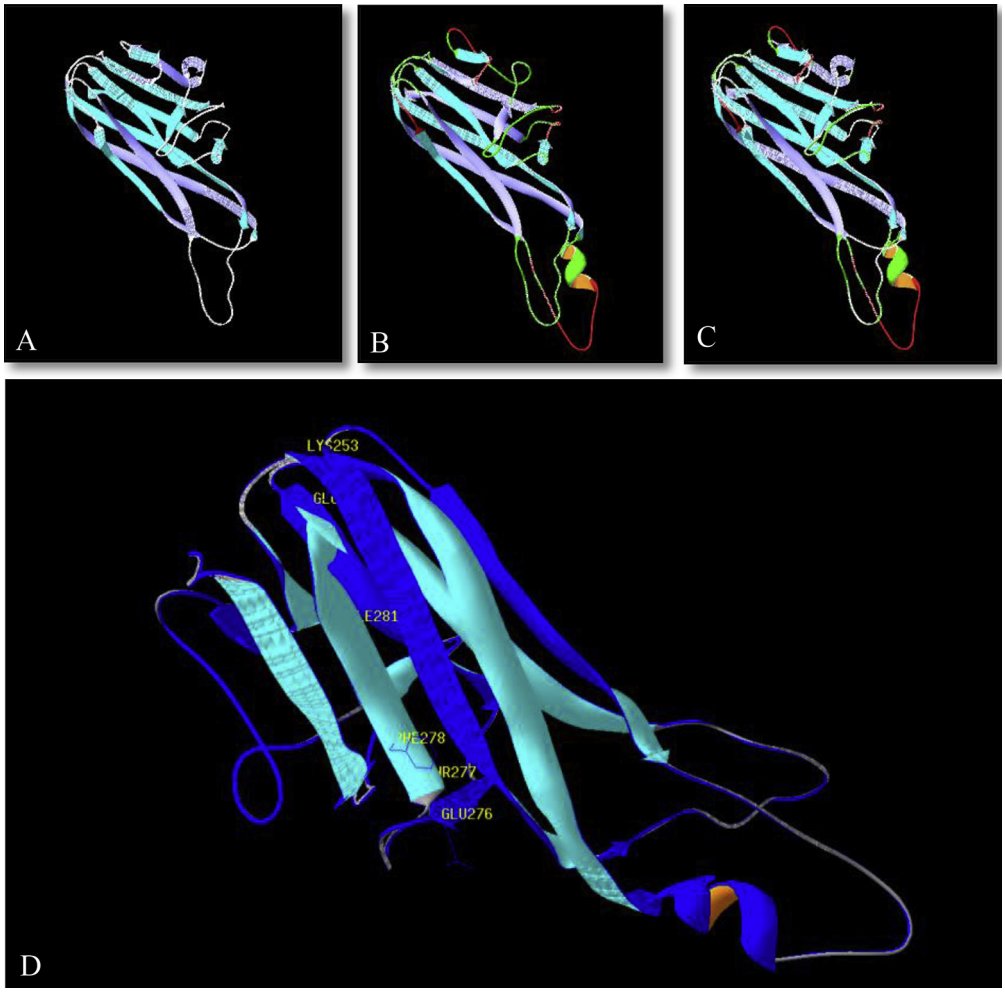

Fig. 6. Three dimensional structure of *Ci*TNF-α. A) Template structure of human TNF superfamily ligand TL1A (2re91B.). B) Homology model of *Ci*TNF-α. C) overlap of target/template structures. D) In the *Ci*TNF-α homology model the positions, including the C-terminal variables aa, of more frequent aminoacid variable sites are reported. All the variable aminoacids are closed and in an external region.

All these polymorphic proteins belong to the immune system and our work extended the diversity phenomenon to another immune molecule. The existence of genomic rearrangement, or alternative splicing, has also been demonstrated, as for example in *Drosophila* Dscam (Schmucker et al., 2000) or ascidian fester (Nyholm et al., 2006).

Neutrality tests gave information about possible effects of selective pressure on TNF-α protein domains or on positive, negative or neutral selection that could work on amino acids.

A bioinformatic analysis performed on data released by Pallavicini et al. (2008) concluded that polymorphism within myticin C loci was driven by positive selection, indicating adaptive evolution of certain amino acids (Padhi and Verghese, 2008). Similar analysis performed by the same authors, with an identical conclusion, concerned shrimp penaeidins (Padhi et al., 2007). In both cases, the hypothesis suggested that interaction with surrounding pathogens in the changing environment caused molecular adaptation.

Recent study on polymorphism conducted by DGGE on Macrophage inhibition Factor (MIF) within and between *M. galloprovincialis* populations of distant geographic origins showed that numerous mutation points have been observed within the Mg-MIF ORF, defining 11 amino acid variants within the mussels from Palavas (France) and 14 amino acid variants within the mussels from Palermo-Italy (Parisi et al., 2012).

Populations under environmental pressure may amplify genetic variability, on which negative or positive selection acts, directing molecular evolution to adaptation. Future similar studies on different populations could help us to understand whether immune-molecules like TNF exposed to environmental pressure will show if a different speed can affect continuously occurring host/parasite/environment relationships.

References

Abrams, E.S., Stanton, V.P., 1992. Use of denaturing gradient gel electrophoresis to study conformational transitions in nucleic acids. Methods Enzymol. 212, 71–104.
Arnold, K., Bordoli, L., Kopp, J., Schwede, T., 2006. The SWISS-MODEL workspace: a web-based environment for protein structure homology modelling. Bioinformatics 22, 195–201.
Bacher, M., Meinhardt, A., Lan, H., Mu, W., Metz, C., Chesney, J., Gemsa, D., Donnelly, T., Atkins, C., Bucala, R., 1998. MIF expression in the rat brain: implications for neuronal function. Mol. Med. 4, 217–230.
Ballarin, L., Cammarata, M., 2016. Lessons in immunity. From Single-cell Organisms to Mammals. Academic Press El Sevier, pp. 1–308.
Benigni, F., Atsumi, T., Calandra, T., Metz, C., Echtenacher, B., Peng, T., Bucala, R., 2000. The proinflammatory mediator macrophage migration inhibitory factor induces glucose catabolism in muscle. J. Clin. Invest 106 (10), 1291–1300.
Bodmer, J.L., Schneider, P., Tschopp, J., 2002. The molecular architecture of the TNF superfamily. Trends Biochem. Sci. 27, 19–26.
Brunetti, R., Gissi, C., Pennati, R., Caicci, F., Gasparini, F., Manni, L., 2015.

Morphological evidence that the molecularly determined *Ciona intestinalis* type A and type B are different species: *Ciona robusta* and *Ciona intestinalis*. J. Zool. Syst. Evol. Res. 53 (3), 186–193.
Cantet, F., Toubiana, M., Parisi, M.G., Sonthi, M., Cammarata, M., Roch, P., 2012. Individual variability of mytimycin gene expression in mussel. Fish Shellfish Immunol.
Charlesworth, A., Ridge, J.A., King, L.A., MacNicol, M.C., MacNicol, A.M., 2002. A novel regulatory element determines the timing of Mos mRNA translation during Xenopus oocyte maturation. EMBO J. 21, 2798–2806.
Charlesworth, A., Wilczynska, A., Thampi, P., Cox, L.L., MacNicol, A.M., 2006. Musashi regulates the temporal order of mRNA translation during Xenopus oocyte maturation. EMBO J. 25, 2792–2801.
Costa, M.M., Dios, S., Alonso-Gutierrez, J., Romero, A., Novoa, B., Figueras, A., 2009. Evidence of high individual diversity on myticin C in mussel (*Mytilus galloprovincialis*). Dev. Comp. Immunol. 33, 162–170.
Diez, B., Pedros-Alio, C., Marsh, T.L., Massana, R., 2001. Application of denaturing gradient gel electrophoresis (DGGE) to study the diversity of marine picoeukaryotic assemblages and comparison of DGGE with other molecular techniques. Appl. Environ. Microbiol. 53, 2942–2951.
Eck, M.J., Sprang, S.R., 1989. The structure of tumor necrosis factor-alpha at 2.6 A resolution. Implications for receptor binding. J. Biol. Chem. 264, 17595–17605.
Fisher, S.G., Lerman, L.S., 1979. Length-independent separation of DNA restriction fragments in two-dimensional gel electrophoresis. Cell 16, 191–200.
Fu, Y.X., Li, W.H., 1993. Statistical tests of neutrality of mutations. Genetics 133 (3), 693–709.
Galli, S.J., Borregaard, N., Wynn Thomas, A., 2011. Phenotypic and functional plasticity of cells of innate immunity: macrophages, mast cells and neutrophils. Nat. Immunol. 12, 1035–1044.
Ge, W., Davis, M.E., Hines, H.C., Irvin, K.M., 1999. Two-allelic DGGE polymorphism detected in the promoter region of the bovine GHR gene. Anim. Genet. 30, 71.
Gestal, C., Costa, M., Figueras, A., Novoa, B., 2007. Analysis of differentially expressed genes in response to bacterial stimulation in hemocytes of the carpet-shell clam Ruditapes decussatus: identification of new antimicrobial peptides. Gene 406, 134–143.
Guex, N., Peitsch, M.C., 1997. SWISS-MODEL and the Swiss-PdbViewer: an environment for comparative protein modeling. Electrophoresis 18, 2714–2723.
Hibino, T., Loza-Coll, M., Messier, C., Majeske, A.J., Cohen, A.H., Terwilliger, D.P., Buckley, K.M., Brockton, V., Nair, S.V., Berney, K., Fugmann, S.D., Anderson, M.K., Pancer, Z., Cameron, R.A., Smith, L.C., Rast, J.P., 2006. The immune gene repertoire encoded in the purple sea urchin genome. Dev. Biol. 300, 349–365.
Imler, J.L., Bulet, P., 2005. Antimicrobial peptides in Drosophila: structures, activities and gene regulation. Chem. Immunol. Allergy 86, 1–21.
Kurn, U., Sommer, F., Hemmrich, G., Bosch, T.C.G., Khalturin, K., 2006. Allorecognition in urochordates: identification of a highly variable complement receptor-like protein expressed in follicle cells of *Ciona*. Dev. Comp. Immunol. 31, 360–371.
Lerman, L.S., Beldjord, C., 1998. Comprehensive Mutation Detection with Denaturing Gradient Gel Electrophoresis. Mutation Detection: A Practical Approach. Oxford University Press, Oxford, pp. 35–59.
Locksley, R.M., Killeen, N., Lenardo, M.J., 2001. TNF and TNF receptor superfamilies: integrating mammalian biology. Cell 104, 487–501.
Muyzer, G., de Waal, E.C., Uitterlinden, A.G., 1993. Profiling of complex microbial populations by denaturing gradient gel electrophoresis analysis of polymerase chain reaction-amplified genes coding for 16S rRNA. Appl. Environ. Microbiol. 59, 695–700.
Nyholm, S.V., Passegue, E., Ludington, W.B., Voskoboynik, A., Mitchel, K., Weissman, I.L., De Tomaso, A.W., 2006. fester, A candidate allorecognition receptor from a primitive chordate. Immunity 25, 163–173.
Padhi, A., Verghese, B., 2008. Molecular diversity and evolution of myticin-C antimicrobial peptide variants in the Mediterranean mussel, Mytilus galloprovincialis. Peptides 29, 1094–1101.
Padhi, A., Verghese, B., Otta, S.K., Varghese, B., Ramu, K., 2007. Adaptive evolution after duplication of penaeidin antimicrobial peptides. Fish. Shellfish Immunol. 23, 553–566.
Pallavicini, A., del Mar Costa, M., Gestal, C., Dreos, R., Figueras, A., Venier, P., Novoa, B., 2008. High sequence variability of myticin transcripts in hemocytes of immune- stimulated mussels suggests ancient host-pathogen interactions. Dev. Comp. Immunol. 32, 213–226.
Parisi, M.G., Li, H., Toubiana, M., Parrinello, N., Cammarata, M., Roch, P., 2009. Polymorphism of mytilin B mRNA is not translated into mature peptide. Mol. Immunol. 46 (3), 384–392.
Parisi, M.G., Toubiana, M., Mangano, V., Parrinello, N., Cammarata, M., Roch, P., 2012. MIF from mussel: coding sequence, phylogeny, polymorphism, 3D model and regulation of expression. Dev. Comp. Immunol. 36, 688–696.
Parrinello, D., Sanfratello, M.A., Vizzini, A., Cammarata, M., 2015. The expression of an immune-related phenoloxidase gene is modulated in Ciona intestinalis ovary, test cells, embryos and larva. J. Exp. Zool. Part B 324, 141–151.
Parrinello, N., Vizzini, A., Arizza, V., Salerno, G., Parrinello, D., Cammarata, M., Giaramita, F.T., Vazzana, M., 2008. Enhanced expression of a cloned and sequenced *Ciona intestinalis* TNFalpha-like (CiTNF alpha) gene during the LPS-induced inflammatory response. Cell Tissue Res. 334, 305–317.
Parrinello, N., Vizzini, A., Salerno, G., Sanfratello, M.A., Cammarata, M., Arizza, V., Vazzana, M., Parrinello, D., 2010. Inflamed adult pharynx tissues and swimming larva of Ciona intestinalis share CiTNFα-producing cells. Cell Tissue Res. 341, 299–311.
Roger, T., Ding, X., Chanson, A.L., Renner, P., Calandra, T., 2007. Regulation of constitutive and microbial pathogen-induced human macrophage migration inhibitory factor (MIF) gene expression. Eur. J. Immunol. 37, 3509–3521.
Royet, J., Reichhart, J.M., Hoffmann, J.A., 2005. Sensing and signaling during infection in Drosophila. Curr. Opin. Immunol. 17, 11–17.
Sampath, P., Mazumder, B., Seshadri, V., 2003. Fox P Transcript-Selective Translational Silencing by Gamma Interferon Is Directed by a Novel Structural Element in the Ceruloplasmin mRNA 3′ Untranslated Region. Mol. Cell Biol. 23, 1509–1519.
Schmucker, D., Clemens, J.C., Shu, H., Worby, C.A., Xiao, J., Muda, M., Dixon, J.E., Zipursky, S.L., 2000. Drosophila Dscam is an axon guidance receptor exhibiting extraordinary molecular diversity. Cell 101, 671–684.
Schwede, T., Kopp, J., Guex, N., Peitsch, M.C., 2003. SWISS-MODEL: An automated protein homology-modeling server. Nucleic Acids Res. 31, 3381–3385.
Sheffield, V.C., Cox, D.R., Lerman, L.S., Myers, R.M., 1989. Attachment of a 40 base-pair G+C-rich sequence (GC-clamp) to genomic DNA fragments by the polymerase chain reaction results in improved detection of single-base changes. Proc. Natl. Acad. Sci. U. S. A. 86, 232–236.
Tajima, F., 1989. Statistical method for testing the neutral mutation hypothesis by DNA polymorphism. Genetics 123, 585–595.
Tauszig, S., Jouanguy, E., Hoffmann, J.A., Imler, J.L., 2000. Toll-related receptors and the control of antimicrobial peptide expression in Drosophila. Proc. Natl. Acad. Sci. U. S. A. 97, 10520–10525.
Van der Gucht, K., Vandekerckhove, T., 2005. Characterization of bacterial communities in four freshwater lakes differing in nutrient load and food web structure. FEMS – Microbiol. Ecol. 205–220.
Ware, C.F., 2003. The TNF superfamily. Cytokine Growth Factor Rev. 14, 181–184.
Watson, F.L., Puttmann-Holgado, R., Thomas, F., Lamar, D.L., Hughes, M., Kondo, M., Rebel, V.I., Schmucker, D., 2005. Extensive diversity of Ig-superfamily proteins in the immune system of insects. Science 309, 1874–1878.
Wu, C.H., McLarty, J.W., 2012. Neural networks and genome informatics. Methods Comput. Biol. Biochem. 1.
Zhang, S.M., Adema, C.M., Kepler, T.B., Loker, E.S., 2004. Diversification of Ig superfamily genes in an invertebrate. Science 305, 251–254.